Analysis of Distributed Pore Closure in Gas-Solid Reactions

The recent random-pore model (Bhatia and Perlmutter, 1980, 1981a; Gavalas, 1980) is further developed to account for distributed pore reaction in gas-solid systems. Numerical solutions for the resulting equations are presented for the case when the reaction is accompanied by an increase in volume of the solid phase. It is shown that in such situations pore closure begins with the smaller pores and progresses to the larger ones. For certain pore size distributions seemingly incomplete conversion is found even when sufficient initial porosity exists so that complete pore closure cannot occur.

S. K. BHATIA

Department of Chemical Engineering
University of Florida
Gainesville, FL 32611

SCOPE

Distributed pore reaction in gas-solid systems is analyzed here by means of the recent random-pore model (Bhatia and Perlmutter, 1980, 1981a; Gavalas, 1980). This represents an extension of the prior model (Bhatia and Perlmutter, 1981a) which assumed a linear concentration gradient of the reactant fluid in the product layer and considered the pore and reaction surface areas to be equal. These assumptions are relaxed in this treatment and it is shown that a variety of experimental observations can be interpreted by the new approach. In particular, for reactions accompanied by an increase in the volume of the solid phase, the role of distributed-pore closure is analyzed and used to explain the gradual approach to the ultimate conversion as is experimentally observed (Hartman and Coughlin, 1976; Ulerich et al., 1978). Prior models have either predicted an abrupt pore closure and cessation of reaction (Georgakis et al., 1979; Bhatia and Perlmutter, 1981a,b), or have introduced an additional fitting parameter in the form of a residual porosity (Hartman and Coughlin, 1976) to simulate the true behavior. It is also demonstrated that apparent incomplete conversion may arise for certain pore size distributions even in the absence of complete pore closure, consistent with recent experimental reports (Bhatia and Perlmutter, 1983a). The new development also predicts changes in the internal surface area with conversion (sintering effects not included), a feature not possible with prior models.

CONCLUSIONS AND SIGNIFICANCE

The further development of the random-pore model presented here allows for distributed pore reaction while accounting for differences in the pore and reaction surface areas as well as pore overlaps. Application of the model to reactions involving a decrease in pore volume indicates that smaller pores close first, followed by plugging of the larger ones. As a result of this distributed pore plugging, seemingly incomplete conversions may be anticipated if only a small portion of the total initial pore volume is present in the larger less reactive pores, even when the initial porosity is sufficient to allow complete conversion, a feature observed in a recent experimental study (Bhatia and Perlmutter, 1983a). For systems involving pore closure it is seen that the internal surface area decreases with conversion and the variation is only weakly dependent on the product layer diffusional resistance (and hence on temperature). In addition, over the main stage of the conversion the surface area decreases almost linearly with conversion for the parameter values investigated here, consistent with the observations of Caillet and Harrison (1982).

In recent years there has been considerable interest in the analysis of gas-solid reactions involving pore closure (Hartman and Coughlin, 1976; Ramachandran and Smith, 1977; Chrostowski and Georgakis, 1978; Georgakis et al., 1979; Bhatia and Perlmutter, 1981a,b.) Such reactions have the common feature that the reaction product occupies a larger volume than the reactant consumed, so that the porosity of the solid is gradually reduced with conversion. In such cases often incomplete conversion is noticed and is believed to occur because of pore closure at the particle surface prior to complete conversion, thus sealing off the internal structure from exposure to the gaseous reactant. A well-known example of such behavior is the sulfation of lime by sulfur dioxide, in which the reaction product ($CaSO_4$) occupies roughly three times the volume of CaO consumed.

Present address of S. K. Bhatia: Indian Institute of Technology, Powai, Bombay 400076, India.

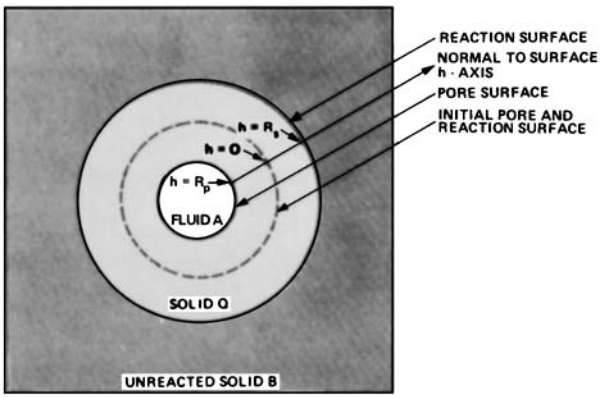

Figure 1. Development of pore and reaction surfaces.

In modeling such systems it has become customary to assume that when the surface porosity, which varies linearly with local conversion as

$$\epsilon = \epsilon_o - (1 - \epsilon_o)X(Z - 1) \tag{1}$$

reduces to zero further reaction does not occur (Ramachandran and Smith, 1977; Georgakis et al., 1979; Bhatia and Perlmutter, 1981a,b). Microscopic examinations (Hartman and Coughlin, 1976), however, show that the porosity never really reduces to zero but takes on a small residual value permitting further reaction to continue, albeit at an extremely slow rate. This prompted Hartman and Coughlin to use the residual porosity as a fitting parameter in their grain model, thus avoiding the abrupt cessation of reaction predicted by the other models. Georgakis et al. (1979) modified the grain model to account for grain expansion as the more voluminous product is formed, but this extension produces the anomaly that the total internal grain surface area increases monotonically while the porosity reduces to zero. Ranade and Harrison (1979) have provided a further modification to allow for sintering as reaction occurs.

In applying their random-pore model to the data of Hartman and Coughlin (1976), Bhatia and Perlmutter (1981b) also use Eq. 1 to predict the maximum conversion at pore closure, but note that in reality pore closure must be distributed with the smaller pores closing first and the larger pores closing later. Thus, a modification of the random-pore model is needed to incorporate this effect. Recently Christman and Edgar (1983) have presented a distributed-pore-size model for limestone sulfation, but neglect pore intersection and overlap. As pointed out elsewhere (Bhatia and Perlmutter, 1983b), it is important in general to include pore overlap, for otherwise in the limit of reaction control the model predicts a monotonically increasing reaction rate as the reaction surface grows with conversion.

More recent experimental results on the reaction between carbon dioxide and lime (Bhatia and Perlmutter, 1983a), however, showed incomplete conversion even when pore diffusion resistances were negligible and sufficient initial porosity existed for the reaction to reach completion. Inspection of the pore size distribution of the reactants however showed that the bulk of the porosity existed in small pores of a narrow size range, with a small amount of pore volume in larger pores of a wide size range. Incomplete conversion was then attributed to closure of the smaller pores, with the large pores being much less active and showing only a small amount of residual reactivity.

In this paper the random-pore model (Bhatia and Perlmutter, 1980, 1981a,b; Gavalas, 1980) is further developed to account for distributed pore closure. Pore overlap is allowed for as before by assuming the pore and reaction surfaces to be randomly distributed. In addition, it is shown that incomplete conversion with a small residual reactivity is consistent with the viewpoint which considers the larger, less reactive pores to be the only available ones at high enough conversion. While in this paper we analyze pore closure, it may be noted that the model is more general and can be used as well when $Z < 1$. Also, since the random pore model has been tested against experimental data in the previous publications referred to, no explicit comparison of this development with experiment is made. Finally, pore diffusion is considered rapid, so that the governing resistances are those of chemical reaction and product layer diffusion, as observed (Bhatia and Perlmutter, 1983a) for the CO_2–lime reaction. The extension to include the pore diffusion resistance is readily accomplished using the well-known effective diffusivity representation (Satterfield, 1970), as shown elsewhere (Bhatia and Perlmutter, 1981a,b).

MODEL DEVELOPMENT

Consider the irreversible reaction of gas A with solid B according to the stoichiometry $aA(g) + bB(s) \rightarrow pP(g) + pQ(s)$. As before, consider the reaction to be initiated on pores of solid B, assumed cylindrical in shape, with the result that as B is consumed a reaction surface moves into the unreacted solid leaving behind a layer of product Q. If the product Q occupies a larger volume than the reactant B consumed, the pore surface moves inward as shown in Figure 1. It is assumed as before (Bhatia and Perlmutter, 1983b), that the pore and reaction surfaces remain cylindrical as reaction proceeds, and diffusion of the reactant fluid A occurs undimensionally between them always along the h direction for any pore.

Focusing on pores of initial size r_o, then all points a distance h away from the original pore surface form contours of constant concentration (Bhatia and Perlmutter, 1983b), so that steady-state conservation of A in the product layer associated with these pores gives

$$\left[\frac{\partial}{\partial h}\left(S\frac{\partial C}{\partial h}\right)\right]_{r_o} = 0; \quad R_p \le h \le R_s \tag{2}$$

where $S(h,r_o)dr_o$ is the surface area of the iso-concentration contour at location h, for all pores of initial size in the interval $[r_o, r_o + dr_o]$. Assuming that all reaction surfaces of radius R_s (which must correspond to the same initial pore size) have the same concentration C_s of species A, integration of Eq. 2 subject to the boundary conditions

$$C = C_A \text{ at } h = R_p \tag{3}$$

and surface reaction with rate constant k_s at $h = R_s$, i.e.

$$\frac{\partial R_s}{\partial t} = k_s C_s = -\frac{D_p M b}{\rho a}\left(\frac{\partial C}{\partial h}\right) \text{ at } h = R_s \tag{4}$$

gives

$$\frac{\partial R_s}{\partial t} = \frac{k_s C_A}{1 + \dfrac{k_s \rho a S(R_s, r_o)}{M b D_p}\displaystyle\int_{R_p}^{R_s} \frac{dh}{S(h,r_o)}} \tag{5}$$

where the constancy of r_o is implicit in the partial derivatives.

Since the reaction and pore surfaces always move in the normal direction, $S(h,r_o)dr_o$ must also correspond to the value of the area of the reaction surface for pores of initial size r_o when it is at position h for $0 \le h \le R_s$, and to the value of the pore surface when it is at h for $R_p \le h \le 0$.

Equation 5 can be used to obtain the growth of the reaction surface corresponding to any pore of initial size r_o. However, it is necessary first to relate the surface area $S(h,r_o)$ to the geometry of the moving pore and reaction surfaces. To this end we assume as before (Bhatia and Perlmutter, 1980, 1981a, 1983b), that the reaction surface is comprised of a system of randomly overlapping growing cylinders of arbitrary size distribution. If $V_{E>R}$ is the total volume of the nonoverlapping cylinders of radius larger than R per unit volume of space, one may write (Gavalas, 1980)

$$V_{>R} = 1 - e^{-V_{E>R}} \tag{6}$$

where $V_{>R}$ is the overlapped volume for surfaces of radius larger than R. Differentiating Eq. 6, as the reaction surfaces grow

$$\frac{\partial V_{>R}}{\partial t} = (1 - V_{>R}) \frac{\partial V_{E>R}}{\partial t} \tag{7}$$

Since the pore volume is assumed randomly distributed in the solid, we may write

$$\frac{\partial V_{>R}}{\partial t} = \left[\int_R^\infty \left(\frac{\partial S_{>R'}}{\partial R'} \right) \left(\frac{dR'}{dt} \right) dR' \right] + V_{<R} \frac{\partial V_{E>R}}{\partial t} \tag{8}$$

where $(\partial S_{>R'}/\partial R')dR'$ in the integrand represents the area of reaction surfaces having radius in the range $[R',R' + dR']$, and the second term acounts for the growth at intersections of pores larger than R into pores smaller than R. Substituting Eq. 8 into Eq. 7 provides

$$\left[\int_R^\infty \left(\frac{\partial S_{>R'}}{\partial R'} \right) \left(\frac{dR'}{dt} \right) dR' \right] - (1 - V_s) \frac{\partial V_{E>R}}{\partial t} = 0 \tag{9}$$

where V_s represents the total overlapped volume enclosed by reaction surfaces. Now,

$$\frac{\partial V_{E>R}}{\partial t} = \int_R^\infty \left(\frac{\partial S_{E>R'}}{\partial R'} \right) \left(\frac{dR'}{dt} \right) dR' \tag{10}$$

so that

$$\int_R^\infty \left[\frac{\partial S_{>R'}}{\partial R'} - (1 - V_s) \frac{\partial S_{E>R'}}{\partial R'} \right] \left(\frac{dR'}{dt} \right) dR' = 0 \tag{11}$$

But since the growth rate dR'/dt is in general an arbitrary function of R'

$$\frac{\partial S_{>R'}}{\partial R'} = (1 - V_s) \frac{\partial S_{E>R'}}{\partial R'} \tag{12}$$

which relates overlapped and nonoverlapped areas of reaction surfaces of radius larger than R'. Since for each R' there corresponds at any time a unique r_o and vice versa, Eq. 12 yields

$$S(R_s(r_o,t),r_o) = (1 - V_s) S_E(R_s(r_o,t),r_o) \tag{13}$$

where $S_E(R_s(r_o,t),r_o)dr_o$ represents the area of nonoverlapped surfaces at time t, of initial radii in the range $[r_o,r_o + dr_o]$. Equation 13 therefore can be written as

$$S(R_s(r_o,t),r_o) = 2\pi R_s f(r_o)(1 - V_s) \tag{14}$$

where $f(r_o)dr_o$ is the length of nonoverlapped pores of initial radius in the interval $[r_o,r_o + dr_o]$. Since initially the overlapping surfaces must correspond with the pore surface

$$1 - V_s = (1 - X)(1 - \epsilon_o) \tag{15}$$

So that Eq. 14 becomes

$$S(R_s(r_o,t),r_o) = 2\pi R_s (1 - X)(1 - \epsilon_o) f(r_o) \tag{16}$$

Similarly, considering the pore surfaces of initial radius in the range $[r_o,r_o + dr_o]$ as being moving overlapping cylinders gives

$$S(R_p(r_o,t),r_o) = 2\pi R_p (1 - V_p) f(r_o) \tag{17}$$

or, since $V_p = \epsilon$, Eqs. 1 and 17 yield

$$S(R_p(r_o,t),r_o) = 2\pi R_p [1 + (Z - 1)X](1 - \epsilon_o) f(r_o) \tag{18}$$

Defining the transformation

$$y = 2\pi f(r_o) \int_{R_p}^{R_s} \frac{dh}{S(h,r_o)} \tag{19}$$

Eqs. 5, 16, 18, and 19 combine to give

$$\frac{\partial R_s}{\partial t} = \frac{k_s C_A}{1 + \dfrac{k_s \rho a (1 - \epsilon_o)(1 - X) R_s y}{MbD_p}} \tag{20}$$

and

$$\frac{\partial y}{\partial t} = \left[\frac{1}{R_s(1 - X)} \left(\frac{\partial R_s}{\partial t} \right) - \frac{1}{R_p[1 + (Z - 1)X]} \left(\frac{\partial R_p}{\partial t} \right) \right] \frac{1}{(1 - \epsilon_o)} \tag{21}$$

It is now necessary to relate R_p and X to R_s in order to obtain the conversion-time behavior using Eqs. 20 and 21. To obtain the relation between R_s and R_p, assume as before (Bhatia and Perlmutter 1980, 1981a, 1983b) that the reaction and pore surfaces are comprised of randomly overlapping cylinders of arbitrary size distribution. It is then possible to write (Bhatia and Perlmutter, 1980; Gavalas, 1980) using the properties of randomly overlapping surfaces as in Eq. 6

$$V_s = 1 - e^{-V_{sE}} \tag{22}$$

and

$$V_p = 1 - e^{-V_{pE}} \tag{23}$$

where V_{sE} and V_{pE} are the volumes enclosed by the nonoverlapped cylinders corresponding to the reaction and pore surfaces respectively. Now, as reaction occurs

$$\frac{dV_p}{dt} = -(Z - 1) \frac{dV_s}{dt} \tag{24}$$

and combining this with Eqs. 22 and 23

$$(1 - V_p) \frac{dV_{pE}}{dt} = -(Z - 1)(1 - V_s) \frac{dV_{sE}}{dt} \tag{25}$$

In Eq. 25 V_{pE} and V_{sE} may be rewritten in terms of the length size distribution function $f(r_o)$ to yield

$$(1 - V_p) \int_0^\infty 2\pi f(r_o) R_p \frac{\partial R_p}{\partial t} dr_o = -(Z - 1)(1 - V_s) \int_0^\infty 2\pi f(r_o) R_s \frac{\partial R_s}{\partial t} dr_o \tag{26}$$

and, since $\partial R_s/\partial t$ is in general arbitrary and $R_p = R_p(R_s,r_o)$, Eq. 26 reduces to

$$(1 - V_p) R_p \frac{\partial R_p}{\partial t} = -(Z - 1)(1 - V_s) R_s \frac{\partial R_s}{\partial t} \tag{27}$$

Recognizing that $V_p = \epsilon$, and combining Eq. 27 with Eqs. 1 and 15

$$\frac{\partial R_p}{\partial t} = -\frac{(Z - 1)(1 - X) R_s}{[1 + (Z - 1)X] R_p} \left(\frac{\partial R_s}{\partial t} \right) \tag{28}$$

So that Eq. 21 transforms to

$$\frac{\partial y}{\partial t} = \left[\frac{1}{R_s(1 - X)} + \frac{(Z - 1)(1 - X) R_s}{R_p^2[1 + (Z - 1)X]^2} \right] \frac{1}{(1 - \epsilon_o)} \left(\frac{\partial R_s}{\partial t} \right) \tag{29}$$

where $\partial R_s/\partial t$ is expressed by Eq. 20. To relate X to R_s we combine Eqs. 15 and 22 to yield

$$X = 1 - \frac{e^{-V_{sE}}}{(1 - \epsilon_o)} \tag{30}$$

Now, since

$$V_{sE} = \int_0^\infty \pi R_s^2(r_o,t) f(r_o) dr_o \tag{31}$$

Eq. 30 is reexpressed as

$$X = 1 - \frac{\exp\left[- \int_0^\infty \pi R_s^2(r_o,t) f(r_o) dr_o \right]}{(1 - \epsilon_o)} \tag{32}$$

providing the needed relation. Equations 20, 28, 29, and 32 must be simultaneously solved to obtain the conversion-time behavior, in the absence of intraparticle concentration gradients. In the presence of such effects these equations must be considered as point relations to be solved in conjunction with the intraparticle effective diffusion equation as in Bhatia and Perlmutter (1981a). In the present work, however, we confine our discussion to the above equations since the addition of the intraparticle diffusion effect is a well-explored refinement.

In dimensionless form, Eqs. 20, 28, 29 and 32 may be written as

$$\frac{\partial \eta_s}{\partial \tau} = \frac{1}{1 + \beta \eta_s y(1 - X)} \tag{33}$$

$$\frac{\partial \eta_p}{\partial \tau} = -\frac{(Z-1)(1-X)\eta_s}{[1 + (Z-1)X]\eta_p}\left(\frac{\partial \eta_s}{\partial \tau}\right) \tag{34}$$

$$\frac{\partial y}{\partial \tau} = \left[\frac{1}{\eta_s(1-X)} + \frac{(Z-1)(1-X)\eta_s}{[1 + (Z-1)X]^2\eta_p^2}\right]\frac{1}{(1-\epsilon_o)}\left(\frac{\partial \eta_s}{\partial \tau}\right) \tag{35}$$

and

$$X = 1 - \frac{\exp\left[-\int_0^\infty \eta_s^2 \pi \mu_o^3 f(a_o) da_o\right]}{(1-\epsilon_o)} \tag{36}$$

with the initial conditions

$$\eta_s = \eta_p = a_o, \quad y = 0 \text{ at } \tau = 0 \tag{37}$$

In comparison with the prior development (Bhatia and Perlmutter, 1981a) of the random-pore model for thin product layers, the new equations above contain the same parameters β, Z, and ϵ_o, but require the microscopic details of the pore size distribution $f(r_o)$, in place of the macroscopic property $\psi(= 4\pi L_E/S_{Eo}^2)$. This adds to the computational complexity since the evaluation of the integral in Eq. 36 by the use of a Gaussian quadrature or other discretizing procedure requires the solution of Eqs. 33–35 simultaneously at each of the grid points, greatly increasing the number of ordinary differential equations (ODE's) to be solved. Thus, the improved versatility of the new approach in describing distributed pore reaction is accompanied by the increased computational difficulty introduced by the use of the complete pore size distribution function.

Uniform Pore Size Distribution

In the event of a uniform pore size distribution $f(r_o)$ takes on the form of the Dirac delta function

$$f(r_o) = L_E \delta(r_o - \mu_o) \tag{38}$$

and the initial porosity is, using Eq. 23,

$$\epsilon_o = 1 - e^{-\pi L_E \mu_o^2} \tag{39}$$

Substitution of Eqs. 38 and 39 into Eq. 32 yields

$$-\ln(1-X) = \pi L_E \mu_o^2 \left(\frac{R_s^2}{\mu_o^2} - 1\right) \tag{40}$$

Defining

$$\psi = \frac{4\pi L_E}{S_{Eo}^2} \tag{41}$$

and since

$$S_{Eo} = 2\pi \mu_o L_E \tag{42}$$

Eq. 40 provides

$$R_s = \mu_o \sqrt{1 - \psi \ln(1-X)} \tag{43}$$

Substituting Eq. 43 into Eq. 28 and integrating,

$$R_p = \mu_o \sqrt{1 - \psi \ln[1 + (Z-1)X]} \tag{44}$$

Integration of Eq. 17 provides

$$S_o = 2\pi \mu_o L_E (1 - \epsilon_o) \tag{45}$$

Differentiating Eq. 40 and combining with Eqs. 20 and 41–45

$$\frac{dX}{dt} = \frac{k_s C_A S_o (1-X)\sqrt{1 - \psi \ln(1-X)}}{(1-\epsilon_o)\left[1 + \dfrac{k_s \rho a (1-\epsilon_o)(1-X)\sqrt{1 - \psi \ln(1-X)}}{MbD_p S_o}[2\pi \mu_o^2 L_E (1-\epsilon_o) y]\right]} \tag{46}$$

while Eqs. 29 and 40–45 combine to yield

$$\frac{dy}{dX} = \left[\frac{1}{(1-X)^2[1 - \psi \ln(1-X)]} + \frac{(Z-1)}{[1 + (Z-1)X]^2[1 - \psi \ln[1 + (Z-1)X]]}\right] \times \frac{1}{2\pi \mu_o^2 L_E (1-\epsilon_o)} \tag{47}$$

Equations 46 and 47 are in complete agreement with the prior result (Bhatia and Perlmutter, 1983b) for the reaction of a uniform pore-sized solid, demonstrating the consistency of this new development in that limit.

RESULTS AND DISCUSSION

In order to obtain conversion-time behavior for a given set of parameter values it is necessary to solve Eqs. 33–37 simultaneously; however, an analytical solution does not appear to be possible in light of the nonlinear nature of the system. A numerical scheme involving a Gaussian quadrature procedure for the evaluation of the integral in Eq. 36, and a Runge-Kutta method for solving Eqs. 33–35 at the grid points was therefore adopted. In order to avoid stiffness as pore closure occurred, a moving grid procedure was devised in which only pores larger than a chosen minimum size contributed to reaction. Numerical experiments showed that for the pore size distributions considered here good convergence was obtained with 10 or more quadrature points, and a minimum pore size η_p of about 0.025.

Comparison with Prior Model

To compare the conversion-time predictions of the new model with those of the previous thin layer result (Bhatia and Perlmutter, 1981a), a log normal length size distribution of the nonoverlapped pore system

$$f(a_o) = \frac{b e^{-(\ln a_o)^2/2\sigma^2}}{\pi \mu_o^3 a_o} \tag{48}$$

was chosen with $b = 0.228$, $\sigma = 0.52$, and $\mu_o = 400$ Å. This distribution is depicted in Figure 3 as the curve for $X = 0$, showing the pore size varying by a factor of about five in the range in which $f(r_o)$ is appreciable. For this distribution integration gives $S_o = 10$ m^2/cm^3, $\epsilon_o = 0.4$, and $\psi = 2.56$, permitting the relation

$$\beta_1 = \frac{2}{\mu_o S_o}\beta = 5\beta \tag{49}$$

between the parameter β of the new model and the parameter β_1 of the prior result

$$X = 1 - \exp\left(\frac{1}{\psi} - \frac{\left[\sqrt{1 + \beta_1 Z \tau_1} - \left(1 - \dfrac{\beta_1 Z}{\psi}\right)\right]^2 \psi}{\beta_1^2 Z^2}\right) \tag{50}$$

In addition, the dimensionless time τ_1 in Eq. 50 expressed in terms of τ is given as

$$\tau_1 = \frac{S_o \mu_o}{(1-\epsilon_o)}\tau = \frac{2\tau}{3} \tag{51}$$

Figure 2 shows the conversion-time predictions of the two models for Z = 2, and for $\beta = 0$ (the case of reaction control), as well as for $\beta = 10$. For the values of Z and ϵ_o used here, Eq. 1 predicts a maximum conversion of 0.667. The dashed curves in Figure 2 which result from Eq. 50, and which would have otherwise continued to complete conversion, were therefore truncated at $X =$

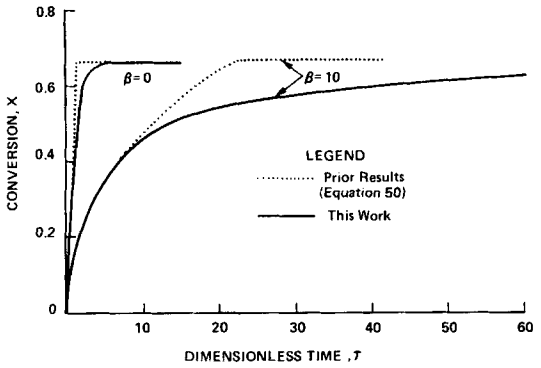

Figure 2. Comparison of conversion predictions for new model with those of Eq. 50.

0.667 after which a horizontal line is depicted, signifying cessation of reaction. The solid lines which represent the solution of the new model Eqs. 33–37, however, asymptotically approach the maximum conversion always showing some reaction proceeding, even close to the maximum conversion, albeit at a very small rate. As mentioned previously, this small reactivity as the solid approaches its maximum conversion has been experimentally noticed (Hartman and Coughlin, 1976; Ulerich et al., 1978) and illustrates the improved characteristics of the new predictions. Over much of the conversion range, however, the two results agree remarkably well, deviating after about 60% of the maximum conversion. This lack of accuracy of the thin layer model beyond about 60% of the maximum conversion has been anticipated earlier (Bhatia and Perlmutter, 1983b) and arises out of the assumption of a linear concentration gradient in the product layer, as well as neglect of progressive closure of the smaller pores. This progressive change in the pore size distribution as predicted by the new approach is shown in Figure 3, which depicts the length size distribution at various levels of conversion for $\beta = 10$. Consistent with the observations of Hartman and Coughlin (1976) and Ulerich et al. (1978), there is a gradual shift in the distribution as the smaller, more reactive pores close preferentially to the larger ones.

Variation of Internal Surface Area

One of the difficulties with many of the existing models for gas-solid reactions is their inability to predict the change in the internal surface area with conversion. The grain models predict the surface area as monotonically increasing even as the porosity reduces to zero, while the prior approximation of the random-pore model does not provide an expression for this variable. Thus, in

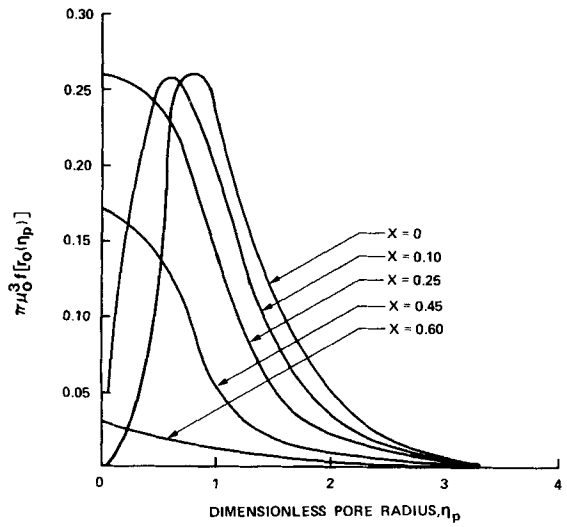

Figure 3. Modification of pore size distribution with conversion.

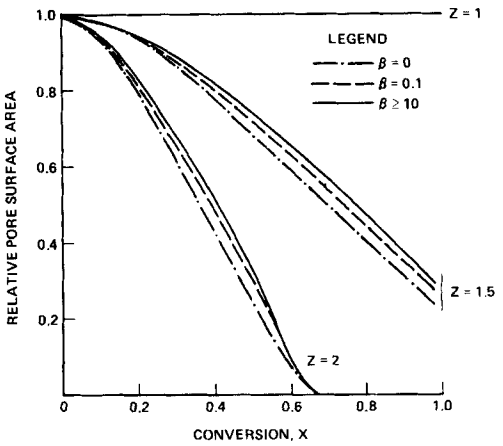

Figure 4. Effect of β and Z on the variation of pore surface area with conversion.

their experiments with the reaction between manganese oxide and hydrogen sulfide, Caillet and Harrison (1982) use an empirical curve fit to relate the change in surface area with conversion. Their data appear to indicate an almost linear drop in surface area with conversion for the system over the main stage of the reaction. In the present model the change in the internal surface with conversion is readily obtained by an integration of Eq. 18, and the results are shown in Figure 4 for the pore length distribution of Eq. 48. For $Z = 1.5$, Eq. 1 predicts that the porosity does not reduce to zero, so that some internal surface must remain at complete conversion. This is readily evident in Figure 4, in which the surface area reduces to zero only for $Z = 2$, whence the maximum conversion is 0.667. This reduction in surface area for the two values of Z larger than unity shown in the figure is consistent with observations such as those of Caillet and Harrison (1982). Indeed the curves of Figure 4 show a good degree of linearity over most of the conversion range, particularly for $Z = 1.5$, in qualitative consistency with the data of Caillet and Harrison. A further interesting feature of the curves in Figure 4 is the relatively small effect of the product layer diffusion parameter β. For $\beta \geq 10$ (effectively product layer diffusion control) the surface area at any conversion is essentially independent of β. The weak dependence on β also signifies only a minor effect of temperature on the surface area, so long as no sintering occurs. The effect of sintering, which can be strongly influenced by temperature (Caillet and Harrison, 1982), is not considered in the present analysis.

Incomplete Conversion

In Figure 2, for $Z = 2$ incomplete conversion is seen, as predicted by Eq. 1, and is due to reduction of the porosity to zero. Recent experimental results (Bhatia and Perlmutter, 1983a), however, show apparent incomplete conversion for the CaO–CO_2 reaction even when sufficient initial porosity exists for the reaction to reach completion. As mentioned previously, this was qualitatively attributed to closure of the small pores, leaving behind only a small amount of pore volume in larger, less reactive pores. To verify that the apparent incomplete conversion does indeed arise from such distributed pore closure, a simulation was performed using the pore size distribution of calcine 2 of Bhatia and Perlmutter (1983a) which had been obtained by decomposing calcium carbonate. Figure 5 shows this distribution, in the form of the pore volume distribution presented in Bhatia and Perlmutter (1983a), which was then differentiated to obtain the function $[\pi\mu_o^3 f(a_o)]$ with μ_o chosen as 0.04 μm. As seen in Figure 5, the porosity of the calcine is 0.53, which according to Eq. 1 should allow essentially complete conversion since $Z = 2.16$ for the reaction. The computed conversion-time behavior for this pore size distribution at various values of β is depicted in Figure 6, showing very little further reaction beyond about 70–75% conversion, in agreement with experimental findings (Bhatia and Perlmutter, 1983a). More detailed compari-

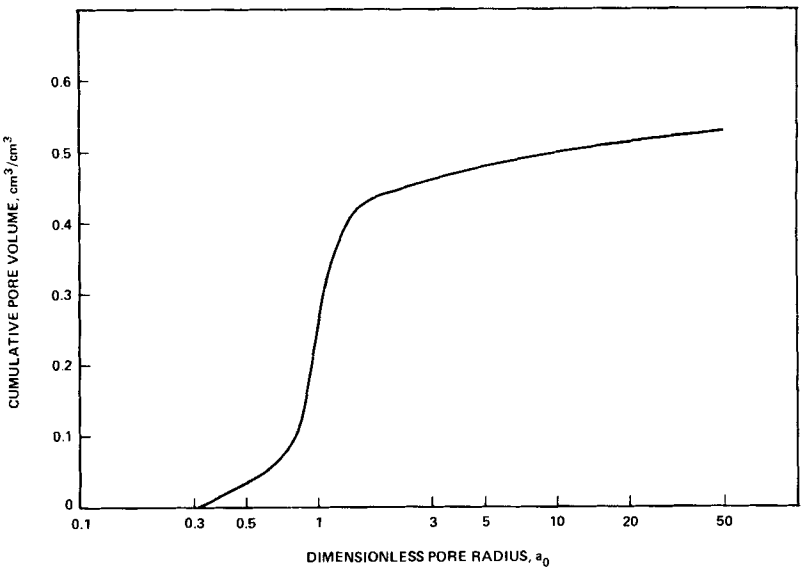

Figure 5. Cumulative pore size distribution used for model calculations.

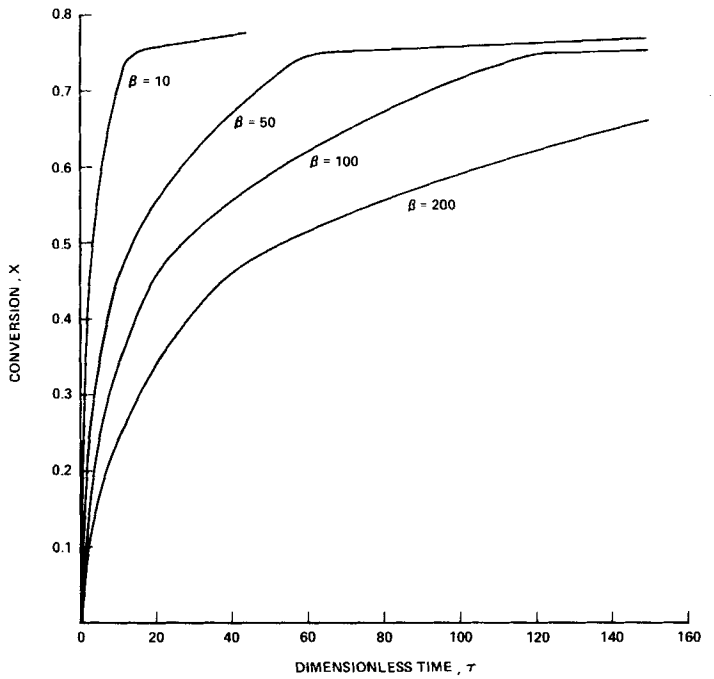

Figure 6. Predicted conversion-time behavior for pore size distribution of Figure 5, at various values of β.

sons with the data were not made because of the large amount of conversion (~12–15%) which occurred during an initial nucleation period. In making the computations, the length size distribution of the calcine was discretized into the four initial sizes $a_o = 0.5, 1, 1.5$, and 10, and the effective values of the function $[\pi\mu_o^3 f(a_o)]$ associated with each size were obtained by matching the first four moments of the discretized system with those of the original distribution. Inspection of the pore sizes at various levels of conversion indicated that the smallest pores ($a_o = 0.5$) had essentially closed by about 45% conversion, with the next pore size ($a_o = 1$) closing at about 74% conversion, leaving behind only the two largest pore sizes still reactive. A drastic reduction in reaction rate to an almost negligibly small level is observed at this conversion, in good agreement with experimental observation (Bhatia and Perlmutter, 1983a). As is evident in Figure 5, there is very little initial porosity beyond about $a_o = 1.5$, so that such pores should show very little reactivity. In addition, $a_o = 1.5$ also corresponds with the point at which there is a rather sudden change in the shape of the pore-size distribution curve, just as in the conversion-time curve. Thus, we see here that the present theory offers a quantitative explanation of the previously observed anomalous behavior in terms of the form of the pore size distribution function. It shows that the time scale of conversion changes as pores progressively close, and in the present case there is a rather drastic change in this scale at about 74% conversion, giving the impression of incomplete conversion. Further conversion may be obtained but would require an impractically large amount of time, a feature also observed in the experiments referred to in this discussion.

NOTATION

a_o = r_o/μ_o, dimensionless initial pore size
a,b = stoichiometric coefficients
C = local concentration of fluid A in product layer
C_A = concentration of fluid A in pores
D_p = effective diffusivity of fluid A in product layer
$f(r_o)$ = length size distribution of nonoverlapped system

h = radial position in product layer, measured from initial pore surface
k_s = rate constant for surface reaction
L_E = total length of nonoverlapped system, per unit volume
M = molecular weight of solid B
p,q = stoichiometric coefficients
r_o = initial pore radius
R = radius of reaction or pore surface
R_p = instantaneous pore radius
R_s = instantaneous radius of reaction surface
$S(h,r_o)dr_o$ = surface area of iso-concentration contour at position h, for pores of initial radii in the interval $[r_o,r_o + dr_o]$
S_E = distribution function for nonoverlapped surface area
$S_{>R}$ = total area of reaction surfaces of radii larger than R
S_o = initial total surface area, per unit volume
S_{Eo} = initial surface area of nonoverlapped system
t = time
V_p = volume enclosed by pore surfaces
V_s = volume enclosed by reaction surfaces
V_{pE} = volume enclosed by nonoverlapped system corresponding to pore surfaces
V_{sE} = volume enclosed by nonoverlapped system corresponding to reaction surfaces
$V_{>R}$ = volume enclosed by reaction surfaces of radii larger than R
$V_{E>R}$ = volume enclosed by nonoverlapped system corresponding to reaction surfaces of radii larger than R
X = conversion
y = transformation defined in Eq. 19
Z = ratio of volume of solid phase after reaction to that before reaction

Greek Letters

β = $k_s\rho a\mu_o(1-\epsilon_o)/MbD_\rho$
β_1 = $2k_s a\rho(1-\epsilon_o)/MbD_bS_o$
ϵ = porosity
ϵ_o = initial porosity
η_s = R_s/μ_o, dimensionless radius of reaction surface
η_p = R_p/μ_o, dimensionless pore radius
μ_o = reference pore radius, mean pore radius
ψ = $4\pi L_E/S_{Eo}^2$
ρ = mass of reactant solid A per unit volume of original solid phase
τ = k_sC_At/μ_o, dimensionless time
τ_1 = $k_sC_AS_ot/(1-\epsilon_o)$, dimensionless time

LITERATURE CITED

Bhatia, S. K., and D. D. Perlmutter, "A Random Pore Model for Fluid-Solid Reactions. I: Isothermal, Kinetic Control," *AIChE J.*, **26**, 379 (1980).
———, "A Random-Pore Model for Fluid-Solid Reactions. II: Diffusion and Transport Effects," *AIChE J.*, **27**, 247 (1981a).
———, "The Effect of Pore Structure on Fluid-Solid Reactions: Application to the SO_2–Lime Reaction," *AIChE J.*, **27**, 226 (1981b).
———, "Effect of the Product Layer on the Kinetics of the CO_2–Lime Reaction," *AIChE J.*, **29**, 79 (1983a).
———, "Unified Treatment of Structural Effects in Fluid-Solid Reactions," *AIChE J.*, **29**, 281 (1983b).
Caillet, D. A., and D. P. Harrison, "Structural Property Variations in the MnO-MnS System," *Chem. Eng. Sci.*, **37**, 625 (1982).
Christman, P. G., and T. F. Edgar, "Distributed Pore-Size Model for Sulfation of Limestone," *AIChE J.*, **29**, 388 (1983).
Chrostowski, J. W., and C. Georgakis, "Pore Plugging Model for Gas-Solid Reactions," 5th Int. Symp. Chem. Reaction Eng., Houston (1978).
Gavalas, G. R., "A Random Capillary Model with Application to Char Gasification at Chemically Controlled Rates," *AIChE J.*, **26**, 577 (1980).
Georgakis, C., D. W. Chang, and J. Szekely, "A Changing Grain Size Model for Gas-Solid Reactions," *Chem. Eng. Sci.*, **34**, 1,072 (1979).
Hartman, M., and R. W. Coughlin, "Reaction of Sulfur Dioxide with Limestone and the Grain Model," *AIChE J.*, **22**, 490 (1976).
Ramachandran, P. A., and J. M. Smith, "A Single-Pore Model for Gas-Solid Non-Catalytic Reactions," *AIChE J.*, **23**, 353 (1977).
Ranade, P. V., and D. P. Harrison, "The Grain Model Applied to Porous Solids with Varying Structural Properties," *Chem. Eng. Sci.*, **34**, 427 (1979).
Satterfield, C. N., *Mass Transfer in Heterogeneous Catalysts*, M.I.T. Press, Cambridge, MA (1970).
Ulerich, N. H., E. P. O'Neill, and D. L. Keairns, "A Thermogravimetric Study of the Effect of Pore Volume-Pore Size Distribution on the Sulfation of Calcined Limestone," *Thermochimica Acta.*, **26**, 269 (1978).

Manuscript received Aug. 19, 1983; revision received Nov. 10, 1983, and accepted Nov. 11.